Plasmonics (2017) 12:717–727
DOI 10.1007/s11468-016-0318-y

Green Synthesis of Gold Nanoparticles with Pectinase: a Highly Selective and Ultra-Sensitive Colorimetric Assay for Mg^{2+}

Yan Zhang[1] · Jingjing Jiang[1] · Min Li[1] · Pengfei Gao[1] · Guomei Zhang[1] · Lihong Shi[1] · Chuan Dong[1] · Shaomin Shuang[1]

Received: 15 March 2016 / Accepted: 29 June 2016 / Published online: 13 July 2016

Abstract A highly selective and ultra-sensitive colorimetric assay has been developed for detecting the magnesium ion (Mg^{2+}) based on pectinase (PE)-protected Au nanoparticles (PE-AuNPs). This is the first study reporting the use of pectinase for green synthesizing gold nanoparticles. Aggregation of PE-AuNPs was induced immediately following the addition of Mg^{2+} ion under Tris-HCl buffer at pH 4.0, yielding a color change from red to blue, and the characteristic surface plasmon resonance (SPR) peak of PE-AuNPs was red-shifted to 665 nm. The effects of parameters such as pH, the amount of PE-AuNPs, and incubation time on the sensitivity of colorimetric assay were investigated in detail. The Mg^{2+}-induced aggregation of PE-AuNPs could be monitored by both the naked eye and UV–vis spectrophotometry. The lowest detection concentration with the naked eye is 0.52 μM. A linear relationship between the absorbance ratio (A_{665}/A_{523}) and Mg^{2+} concentration was observed in two ranges of Mg^{2+} concentration by UV–vis spectrophotometry, including 5.34×10^{-7} μM to 51.4 μM and 5.12×10^{2} μM to 3.19×10^{3} μM. The Mg^{2+} detection limit was determined to be 4.0×10^{-9} μM with UV–vis spectrophotometer. The proposed colorimetric assay possesses a highly selective response for Mg^{2+} over other metal ions. This method has been successfully applied to determine the Mg^{2+} ion in some water samples.

Keywords Gold nanoparticles · Pectinase · Colorimetric assay · Magnesium ion

Introduction

The selective and quantitative detection of metal ions is of great importance in chemical, biological, and environmental science [1]. Magnesium is the eighth most abundant element on the crust of earth and is distributed widely in living bodies such as cells and bones [2, 3]. And it also exerts a large variety of biological functions, such as catalytic roles in enzyme activation or inhibition, regulatory roles by modulating cell proliferation, and cell cycle progression/differentiation [4]. The normal content of magnesium ion (Mg^{2+}) in the human body is 0.8~1.0 mmol L^{-1}. It would have a serious impact on vascular function, endangering the human health, if Mg^{2+} intake is imbalanced in the human body [5, 6]. Therefore, detection and determination techniques of Mg^{2+} have been attracting many scientists in various fields.

Although many methods have been previously reported for Mg^{2+} determination, there are still some challenges for the development of analytical methods for the sensing of Mg^{2+} with simple yet effective features. Over the past few years, several methods to determine the amount of Mg^{2+} such as inductively coupled plasma-mass spectrometry (ICP-MS), atomic absorption spectroscopy (AAS) [7], electrochemical method [8], and fluorescent method [9–11] have been developed, in which fluorescent method is prominent due to its highly sensitivity. The 8-hydroxyquinoline and coumarin derivatives have been reported as effective Mg^{2+} fluorescent indicators [9, 10]. Naruta and coworkers synthesized a

Electronic supplementary material The online version of this article (doi:10.1007/s11468-016-0318-y) contains supplementary material, which is available to authorized users.

✉ Yan Zhang
yanzhang@sxu.edu.cn

✉ Shaomin Shuang
smshuang@sxu.edu.cn

[1] School of Chemistry and Chemical Engineering, Institute of Environmental Science, Shanxi University, Taiyuan 030006, People's Republic of China

porphyrin analogue with an embedded 1,10-phenanthroline moiety and found that this complex could be exploited as a Mg^{2+}-responsive fluorescent chemosensors based on the photo-induced electron transfer (PET) quenching process [11]. However, the reported fluorescent methods demonstrated poor selectivity for Mg^{2+} over Ca^{2+}. So these fluorescent indicators are useful only where the concentrations of Mg^{2+} are much higher than those of Ca^{2+}, as well as the organic indicators could be facile manipulated has been rarely studied and remains a challenging goal [12]. Thus, it is very important to develop a simple, rapid, highly selective, and sensitive methods for Mg^{2+} detection.

Toward achieving this goal, colorimetric sensors are very promising due to their simplicity, cost-effectiveness, and rapid detection times [13]. In particular, gold nanoparticles (AuNPs)-based colorimetric assays attracted a great deal of interest in chemo/biosensing [14, 15], mainly due to the size- and shape-dependent optical properties and large absorption coefficients [16, 17]. Aggregation of the AuNPs will result in color changes of the colloidal solution from red to blue. The clear change in color results can be easily distinguished by the naked eye and not require complicated instruments, making it suitable for point-of-care (POC) diagnostics [18–20]. Compared to fluorimetry sensing strategies, AuNPs-based colorimetric assay show comparable sensitivity because of the high extinction coefficient of AuNPs. Recently Mao's group [21] reported the synthesis of cysteine-capped AuNPs and its colorimetric determination of Mg^{2+}, but the synthesis process requires ligand exchange, resulting in the complexity of the preparation of AuNPs. Many else techniques have also been developed for the synthesis of AuNPs, most of them were often produced by the chemical reduction in the presence of suitable reducing agents and organic stabilizing molecules [22]. The reducing agents in many cases have toxic characteristics, further complicating the application of AuNPs in biosystem [23, 24]. Therefore, the development of new "green" methods to synthesize AuNPs without the reducing agents is an interesting area of study. Recently, the green synthesis of AuNPs have been considerably studied by using harmless biocompatible molecules, such as proteins [25], peptides [26], and amino acids [27] as stabilizing and reducing agents. The use of these benign alternatives is ideal for biological applications because of their assured eco-friendly property [28]. To our knowledge, the development of a rapid, facile, and green approach to synthesize stable, environment-friendly AuNPs still remains a hot research topic.

Microwave (MW) radiation has been reported to be a useful heating source for speeding up chemical reactions in 1986 [29–31]. Thereafter, MW-assisted techniques have attracted considerable attention owing to their distinct and fascinating advantages of uniform heating, rapid reaction, low energy of consumption, cost-effectiveness, and environmentally friendly feature. In this work, we have prepared pectinase (PE)-protected Au nanoparticles (PE-AuNPs) by a simple MW-assisted and green synthetic route. To the best of our knowledge, this is the first report for synthesis pectinase-protected AuNPs through a simple reaction. Further, resultant PE-AuNPs exhibited high selectivity and sensitivity toward Mg^{2+} over other metal ions and due to aggregation of PE-AuNPs caused by Mg^{2+}, resulted in a rapid color change from red to blue. The practicality of this colorimetric assay was further validated by detecting Mg^{2+} in water samples.

Experimental Section

Apparatus and Instruments

The UV–vis absorption spectra were acquired on a U-2910 double-beam UV-visible spectrophotometer (Hitachi, Tokyo Japan) with 1 cm quartz cell. The infrared (IR) spectra were performed on a Nicolet Magna 550 spectrometer (Thermo, Nicolet). Transmission electron microscopy (TEM) images were collected with a JEOL JEM-2100 high-resolution transmission electron microscope (Tokyo, Japan) at an accelerating voltage of 200 kV. The size distribution and zeta potentials of the particles were obtained using a Malvern Instruments Nano-ZS90 Zetasizer. X-ray photoelectron spectroscopy (XPS) data were conducted on an AXIS ULTRA DLD electron spectrometer (Shimadzu, Japan). Thermogravimetric analysis (TGA) were carried out using a Perkin-Elmer Diamond TG/DTA. The pH values of solutions were measured with a pH meter (FE20, Shanghai Mettler Instrument Company, Ltd., China). A Midea M1-L213B domestic microwave oven (Qingdao, China) was used to synthesize the AuNPs.

Chemicals

Hydrogen tetrachloroaurate(III) trihydrate ($HAuCl_4 \cdot 3H_2O$, >99.9 %) was purchased from Aldrich (Milwaukee, WI). Pectinase (PE) was obtained from Sigma (St. Louis, MO). Sodium hydroxide (NaOH, >96 %), tris(hydroxymethyl)aminomethane (Tris), and HCl were from Shanghai Aladdin Reagent Co., Ltd. (Shanghai, China). Magnesium chloride and all other metal salts (analytical reagent grade) were purchased from Beijing Chemical Co. (Beijing, China). Tris-HCl buffers (pH 2.0–10.0) were prepared by mixing 0.05 M Tris and 0.05 M HCl. All chemicals were of analytical reagent grade or better. All solutions were freshly prepared using deionized water having a resistivity of no less than 18.2 MΩ cm^{-1} (Milli-Q, Bedford, MA).

Preparation and Purification of PE-AuNPs

All glassware was thoroughly washed with aqua regia (HNO_3/HCl, 1:3) and rinsed extensively with Milli-Q water prior to use. In a typical microwave-assisted synthesis experiment, briefly, 1.0 mL of 32.5 mg mL^{-1} pectinase solution was added to 1.0 mL of 10 mM $HAuCl_4$ solution at room temperature, and then 0.10 mL of 1.0 M NaOH solution was added. After the mixture was MW radiated (200 W) for 3 min, the color of the solution changed from light-yellow to wine red. Finally, the resulting mixture was cooled slowly to temperature and purified by centrifugation (10,000 rpm, 2 min), the wine red supernatant containing the PE-AuNPs was collected. A cellulose ester dialysis membrane (MWCO 3000 Da) was then used to purify PE-AuNPs. The as-obtained purified PE-AuNPs solution was stored at 4 °C until required for further use. The molar extinction coefficient at 523 nm for (20.0 ± 1.4) nm spherical PE-AuNPs is 8.72×10^8 M^{-1} cm^{-1}; thus, the molar concentration of PE-AuNPs was calculated to be approximately 7.56 nM according to the Lambert Beer's law [32].

Sensitivity and Selectivity Measurements of Mg^{2+} Detection

A high concentration stock solution of Mg^{2+} (1.0 M) was prepared and used to obtain standard solutions with different concentrations through a serial dilution. An aliquot of PE-AuNPs (7.56 nM, 50 μL) was added to Tris-HCl buffers (50 mM, pH 4.0, 2.0 mL). Ten microliters solutions with various concentrations of Mg^{2+} were added and mixed thoroughly, then the mixture was left to react at room temperature for 10 min. Finally, the color change and the corresponding UV–vis absorption spectra were observed. The following metal ions (K^+, Li^+, NH_4^+, Cd^{2+}, Mn^{2+}, Ba^{2+}, Zn^{2+}, Pb^{2+}, Hg^{2+}, Ca^{2+}, Al^{3+}, Cu^{2+}, Fe^{3+}, Co^{2+}, Na^+) at the above-mentioned conditions were used to evaluate the selectivity of this colorimetric assay. In these tests, the concentrations of the other metal ions were 10-fold higher than that of Mg^{2+}. All experiments were performed in triplicate.

Colorimetric Detection of Mg^{2+} in Water Samples

Tap water and lake water samples obtained from our laboratory and the Fen He Lake. All the collected samples were filtered three times through a 0.2-μm membrane to remove any suspended particles before use. One hundred microliters water samples were added into the Tris-HCl buffers (pH 4.0) with 50 μL PE-AuNPs solutions for detection. The standard Mg^{2+} solutions (100 μL) was spiked into the tap water or lake water (100 μL) as stock solutions for the recovery tests. The resulting solutions were further mixed with PE-AuNPs solutions (7.56 nM, 50 μL). After a 10-min incubation period, the UV–vis absorption spectra were recorded.

Results and Discussion

Synthesis and Characterization of PE-AuNPs

Figure 1a portrays the UV–vis absorption spectra of the PE-AuNPs, pectinase, and the mixture of $HAuCl_4$ and pectinase. A strong distinct absorption peak at 523 nm is observed in the spectrum of PE-AuNPs (curve a), which differs from that of pure pectinase (curve b) and MW irradiated pectinase (curve c). In addition, the mixture of $HAuCl_4$ and pectinase after MW irradiation (curve d) displays no distinct absorption peak at 523 nm. Combined the wine red color of the PE-AuNPs solution as sown in the inset of Fig. 1a, which is apparently different with the other yellow solutions, it reveals that the pectinase-protected gold nanoparticles has been successfully obtained. NaOH plays an important role in the synthesis of PE-AuNPs, because it has been reported that the reaction "$4AuCl_4^- + 12OH^- \rightarrow 3O_2 + 6H_2O + 4Au + 16Cl^-$" could release 2.799 E°/V of energy [33]. So Au(III) could be easily reduced to Au(I) or Au(0) by pectinase at basic pH conditions. A simple sketch of the PE-AuNPs preparation process is shown in Scheme 1.

Several protocols were carried out before finding a successful synthetic route. The optimization of the synthesis conditions, including the volume ratio of the initial reagents pectinase to $HAuCl_4$ and the reaction time. Control experiments were carried out with the volume ratio of pectinase to $HAuCl_4$ (PE-to-Au) with 1:3, 1:2, 1:1, 2:1, and 3:1. Figure 1b shows the UV–vis absorption spectra of the products synthesized from different PE-to-Au ratios. The absorption band at 523 nm is strongest at a PE-to-Au ratio 1:1. Figure 1c shows the UV–vis absorption spectra of PE-AuNPs synthesized under different MW irradiation times (1, 2, 3, 4, 5, and 6 min). It is observed that the PE-AuNPs product after MW irradiation 3 min shows higher absorption intensity at 523 nm. One of the most important characteristics of gold nanoparticles is surface plasmon resonance (SPR), which is the result from the collective oscillation of the conduction electrons across the nanoparticle. The gold nanoparticles interacted with incident electromagnetic fields, leading to the excitation of SPR, which prompted intense light absorption at about 520 nm. The SPR absorbance is highly sensitive to the size, sharp, and dielectric constant. The SPR absorbances of PE-AuNPs synthesized under PE-to-Au ratios 1:3, 1:2, 2:1, and 3:1 and MW irradiation times 1, 2, 4, 5, and 6 min, respectively, were weaker than these of PE-to-Au ratio 1:1 and MW irradiation times 3 min. This could be attributed that only very few of PE-AuNPs were formed under PE-to-Au ratios 1:3 and 1:2 and MW irradiation times 1 and 2 min. Larger size PE-AuNPs were synthesized

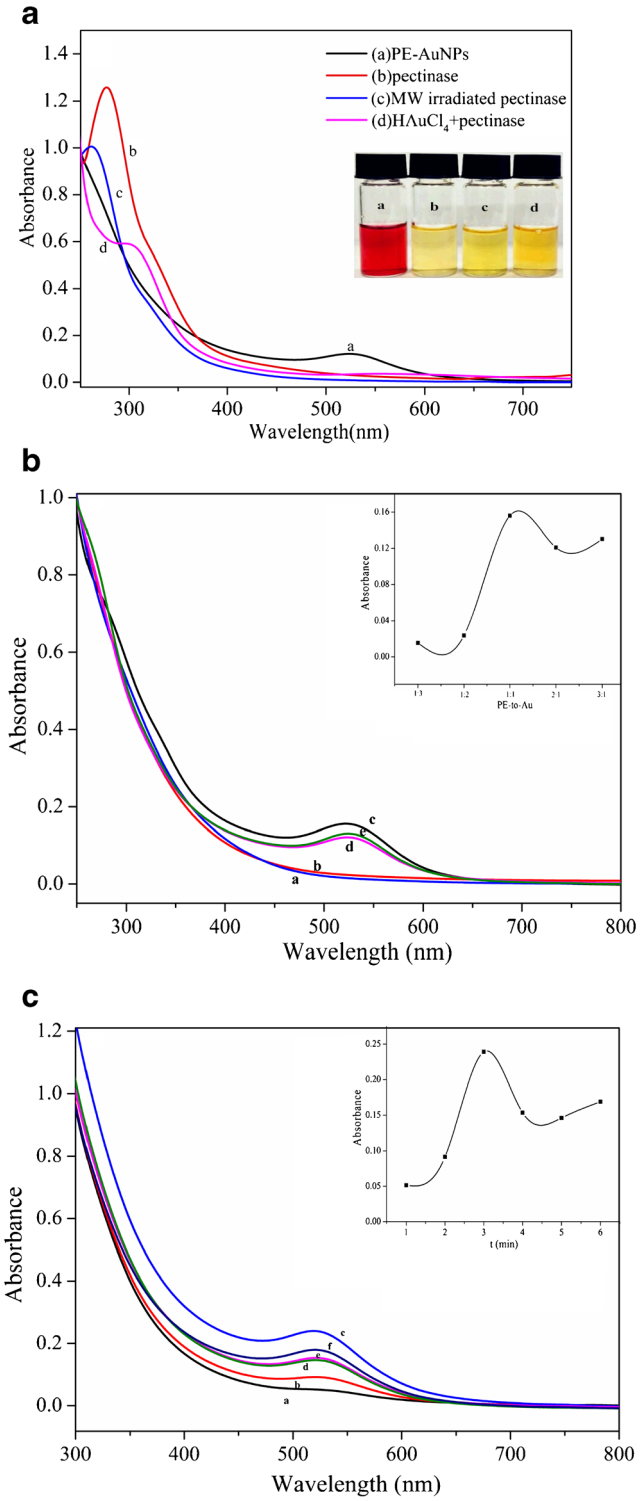

Fig. 1 **a** UV–vis absorption spectra of (*a*) PE-AuNPs, (*b*) pure pectinase, (*c*) MW irradiated pectinase, (*d*) the mixture of $HAuCl_4$ and pectinase after MW irradiation. *Inset* shows the images of these production. **b** PE-AuNPs synthesized in different volume ratios of pectinase to $HAuCl_4$ with 1:3, 1:2, 1:1, 2:1, and 3:1 (curves *a*–*e*). **c** PE-AuNPs synthesized from different MW irradiation times: 1–6 min (curves *a*–*e*)

when PE-to-Au ratio was higher than 1:1 and MW irradiation time was higher than 3 min, which resulted in decreased absorbance at 523 nm and slight red-shift of SPR band. As such, PE-to-Au ratio 1:1 and 3.0 min MW irradiation were applied to our subsequent MW-assisted synthesis of PE-AuNPs.

Various spectroscopic techniques were employed for characterization of the MW-assisted as-synthesized PE-AuNPs product. The typical TEM image of the PE-AuNPs (Fig. 2a) shows an average diameter of about 20.0 ± 1.4 nm. The dynamic light scattering analysis (DLS) of PE-AuNPs shows that the average diameter is 30.1 nm (Fig. 2c), which was slightly larger than that obtained from TEM, mainly due to the fact that TEM measures only metallic core size, whereas in DLS, the average hydrodynamic diameter of PE-AuNPs can also be calculated for the attached water molecules by light scattering through the sample [34, 35].

To evaluate the attachment of PE onto the surface of Au, the surface composition of as-prepared PE-AuNPs was investigated by FT-IR. Figure 3a displays the IR spectra of the pure PE and AuNPs samples. The absorption bands of pectinase at 3413, 2935, 1654, and 1406 cm^{-1} were mainly ascribed to -OH, -CH, -C=O, -C–N stretching vibrations, respectively. Compared with the spectrum of pure pectinase, the main absorption bands of the PE-AuNPs were located at 3429, 2935, 1645, and 1410 cm^{-1}, which indicated that the basic structure of PE still maintained after modifying the PE-AuNPs. It should be noted that these absorption bands of PE-AuNPs were slightly differ from pure pectinase, mainly because PE-AuNPs changes the surface bond force constant of these groups [36]. An obvious peak observed at 2860 cm^{-1} in the spectrum of pectinase, which is attributed to the -H-C=O stretching motions, disappeared in that of PE-AuNPs. Meanwhile, there appeared a distinct absorption band at 1570 cm^{-1} in the spectrum of PE-AuNPs, which is due to the asymmetrical stretching vibration of COO^-. So we proposed that pectinase participated in the $HAuCl_4$ reduction reaction via the -H-C=O group that turned into COO^- group along with the formation of PE-AuNPs. The shift of characteristic peaks of pectinase at 1116, 618, and 520 cm^{-1} confirmed furtherly that pectinase as a stabilizer has been attached on the surface of PE-AuNPs.

TGA is commonly employed to provide the information of the Au core and stabilizer ratio of the gold nanoparticles directly. The PE-AuNPs was estimated by TGA at a heating rate of 10 °C min^{-1} as shown in Fig. 3b. The results show that there was a tiny weight loss at a temperature below 160 °C, which is attributed to evaporation of water. The pectinase was found to decompose and fall off from the surface of PE-AuNPs in the temperature range from 160 to 526 °C, and the weight loss from 526 to 660 °C is attributed to the combustion of pectinase, corresponding to the weight loss of 75.3 wt%, namely, the proportion of gold was 20.8 wt%.

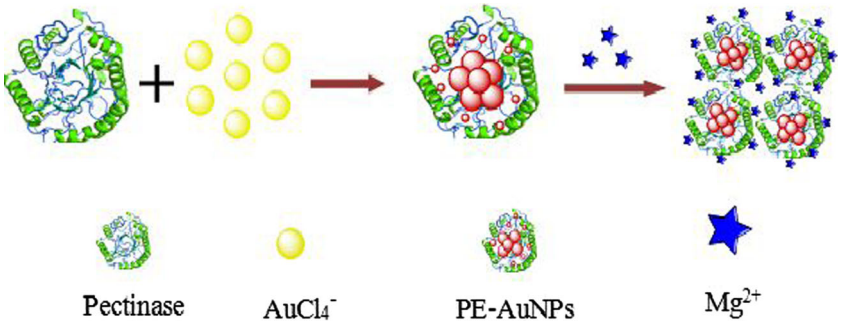

Scheme 1 Schematic representation of the colorimetric assay of Mg^{2+} ion based on the green synthesis of PE-AuNPs

Principle of Colorimetric Assay of Mg^{2+}

Figure 4a shows UV–vis absorption spectra of PE-AuNPs with and without 3.19 mM Mg^{2+}. It is obviously observed that the maximum absorption peak of PE-AuNPs bathochromic-shift from 523 to 665 nm with the addition of Mg^{2+}. The solution color of PE-AuNPs turned to blue from wine red as shown in the inset of Fig. 4a, indicating the formation of PE-AuNPs aggregates. In addition, further evidence for Mg^{2+}-induced aggregation of PE-AuNPs was supported by TEM images and DLS results. Figure 2b shows the TEM image of PE-AuNPs after addition of Mg^{2+} ion. It can be seen that the morphology and sizes of PE-AuNPs were greatly influenced by the addition of Mg^{2+}, which results in a change in their state from monodisperse to polydisperse. The average hydrodynamic diameter of PE-AuNPs was drastically increased from 30.1 to 268 nm by the addition of Mg^{2+} ion, yielding the PE-AuNPs aggregation via the complex formation between PE-AuNPs and Mg^{2+} ions. A zeta potential can be used to derive information concerning the surface charge and the local environment of nanoparticles. In this study, we measured the zeta potentials of PE-AuNPs before and after the addition of Mg^{2+} ion (Fig. S1). A significant increase in the zeta potential from −26.9 to −8.42 mV indicated the augment

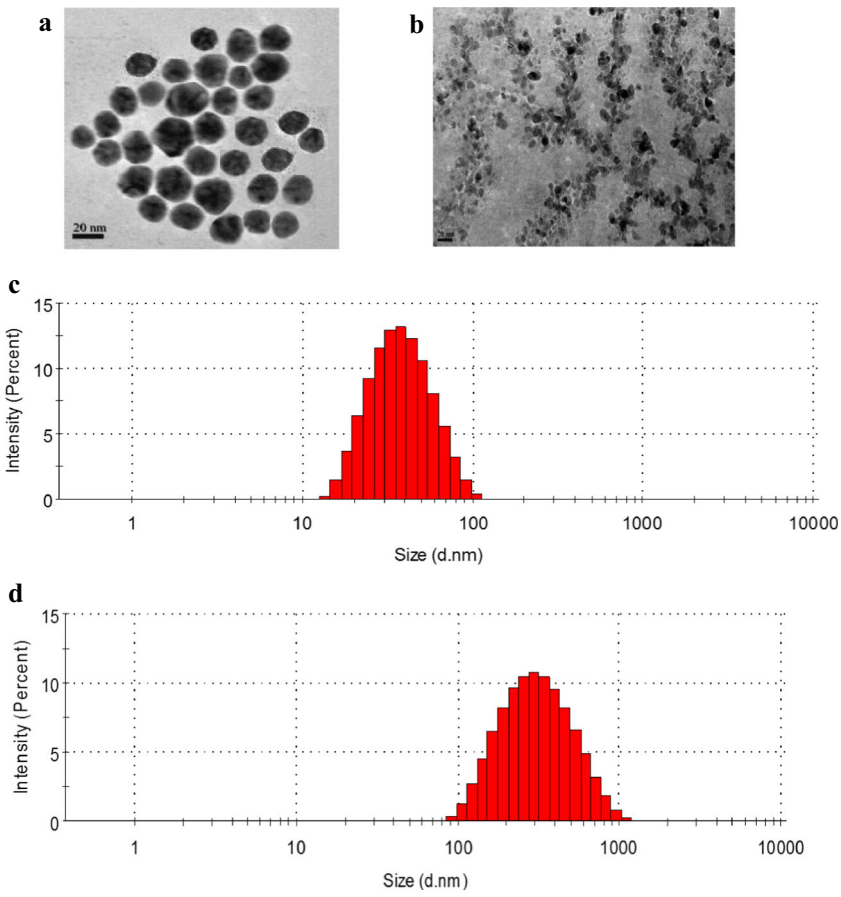

Fig. 2 **a**, **b** TEM images of PE-AuNPs without and with Mg^{2+}. **c**, **d** DLS analysis of without and with Mg^{2+}

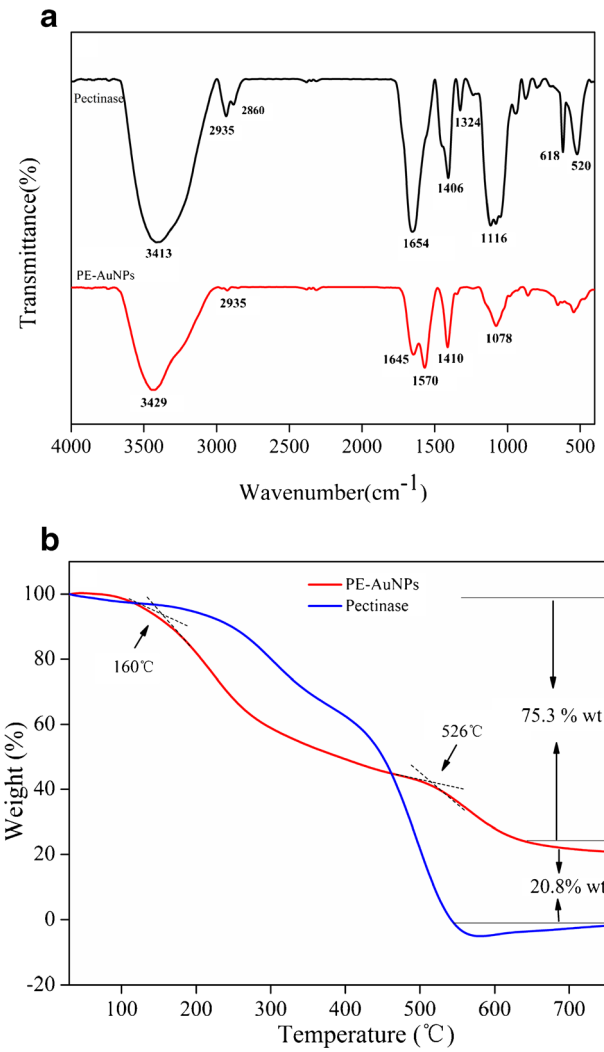

Fig. 3 **a** IR spectra of the pure pectinase (*black line*) and the PE-AuNPs (*red line*). **b** TGA of PE-AuNPs (*red line*) and pectinase (*blue line*)

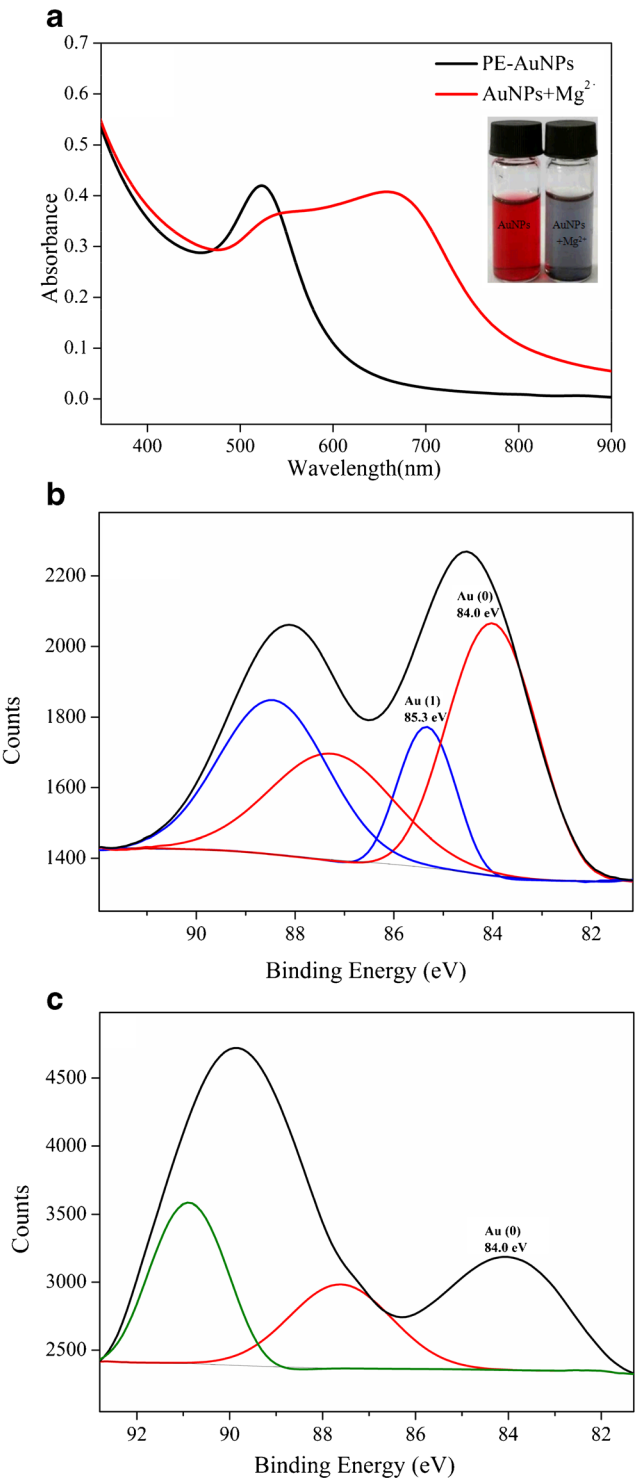

Fig. 4 **a** UV–vis absorption spectra of PE-AuNPs without and with Mg^{2+}; *insert* is images of PE-AuNPs without and with Mg^{2+}. **b**, **c** The XPS measurement of PE-AuNPs before and after the addition of Mg^{2+}

of the surface potential of PE-AuNPs, which also induced aggregation [37]. The TEM, DLS, and zeta potential analysis results were in agreement with the red-shift of the absorption spectra and the color change of PE-AuNPs after the addition of Mg^{2+} ion.

X-ray photoelectron spectroscopy (XPS) analysis was carried out to determine the valence of Au in the PE-AuNPs. The XPS survey spectrum (Fig. 4b) shows two prominent peaks at about 84.5 and 88.0 eV (black curve), which are assigned to Au $4f_{7/2}$ and Au $4f_{5/2}$ for PE-AuNPs, respectively. Then the Au 4f spectrum of the PE-AuNPs could be further deconvoluted into two distinct components (red and blue curves) centered at binding energies of 84.0 and 85.3 eV, which could be identified as Au(0) and Au(I)[38], respectively. These two bands indicated that the most of the gold within the nanoparticles is Au(0), and with a handful of Au(I) surrounded by pectinase, which might stabilize the PE-AuNPs. As shown in Fig. 4c, upon interaction with Mg^{2+}, the peak area for Au(I) in the PE-AuNPs disappeared greatly, illustrating that Mg^{2+} induced further reduction of Au(I) to Au(0), then aggregation of gold nanoparticles occurred. This is consistent with the above research results. And this

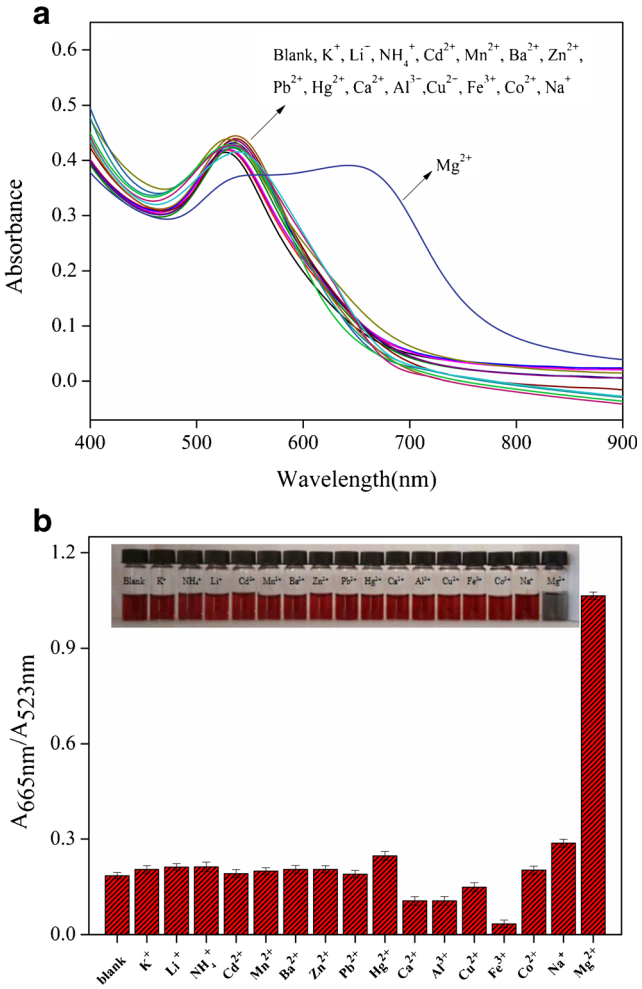

Fig. 5 Selectivity of the colorimetric assay. **a** UV-visible absorption spectra of PE-AuNPs before and after the addition of various metal ions (K^+, Li^+, NH_4^+, Cd^{2+}, Mn^{2+}, Ba^{2+}, Zn^{2+}, Pb^{2+}, Hg^{2+}, Ca^{2+}, Al^{3+}, Cu^{2+}, Fe^{3+}, Co^{2+}, Na^+, Mg^{2+}). **b** The plot of A_{665}/A_{523} versus various metal ions. *Inset* is the corresponding photographic images of PE-AuNPs without and with various metal ions

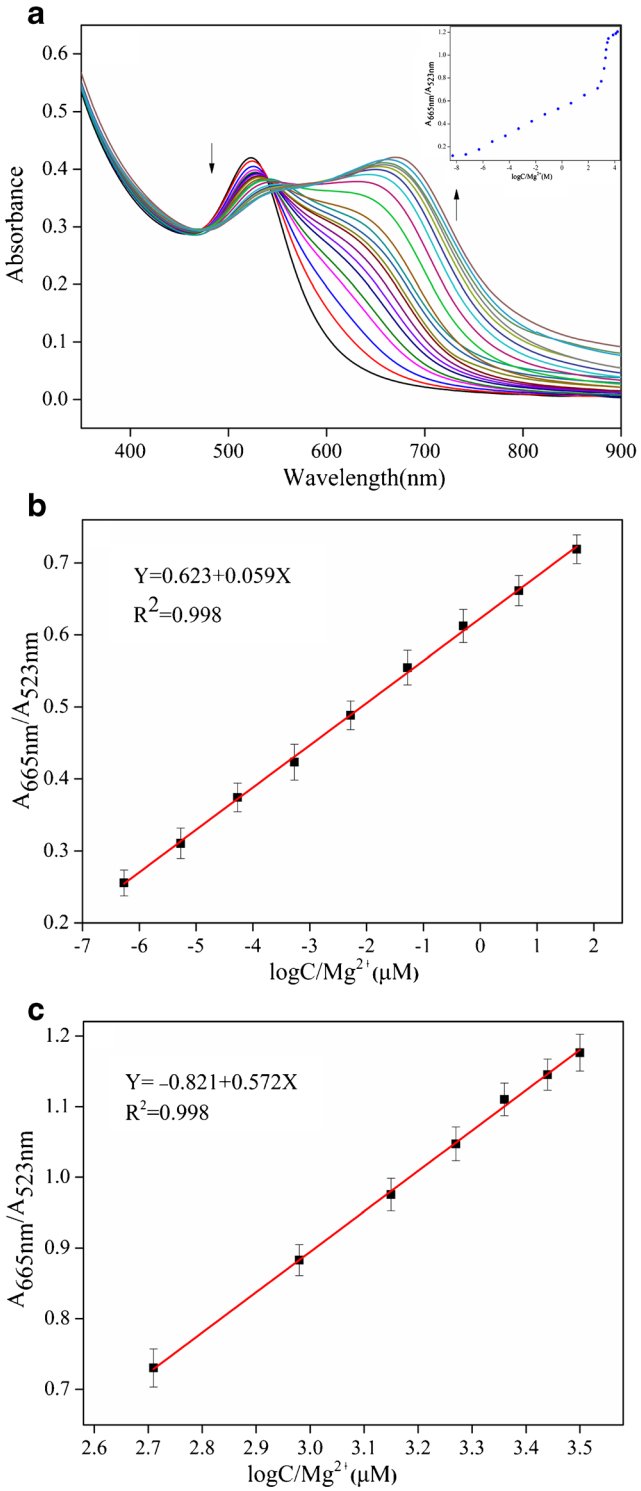

Fig. 6 **a** UV–vis absorption spectra of PE-AuNPs after addition of various concentrations of Mg^{2+}. *Insert* is the absorbance ratio (A_{665}/A_{523}) versus the concentration of Mg^{2+}. **b**, **c** There were two linear relationships between the absorbance ratio (A_{665}/A_{523}) and Mg^{2+} concentration

phenomenon can be further reflected in the scheme of the colorimetric assay of Mg^{2+} ion (Scheme 1).

Optimization of Colorimetric Assay of Mg^{2+}

Since the electrostatic repulsion plays an important role on the dispersion of AuNPs, parameters (e.g., solution pH, incubation time, the amount of AuNPs, etc.) that affect the electrostatic repulsion may have effects on the aggregation behavior of PE-AuNPs [15]. Thus, the effect of these parameters on UV–vis absorption spectra of PE-AuNPs upon adding Mg^{2+} was investigated in this study. With the increase of the concentration of Mg^{2+}, the absorbance of PE-AuNPs at 523 nm decreases gradually and the absorbance at longer wavelength (665 nm) correspondingly increases. So a systematic study was performed by monitoring the ratio of absorbance values at 665 and 523 nm (A_{665}/A_{523}). A lower absorbance ratio indicates that PE-AuNPs disperse well in the solution, and a greater

Table 1 Comparison of this work with some established Mg^{2+} detection methods

Reagents	Methods	Analytical range (μM)	Detection limit (μM)	Ref.
Coumarin derivative	Fluorimetry	100–6000	–	10
4-(1-Naphthaleneacetamido) benzo-15-crown-5	Fluorimetry	10–125	–	3
KCM-1 (single molecular multianalyte)	Fluorimetry	10^3–10^4	–	39
8-Hydroxyquinoline derivatives	Fluorimetry	7.4×10^{-3}–15.4×10^{-3}	–	9
Coumarin chromoionophore	Colorimetry	5.18–4.58×10^2	5.18	40
Calix[4]arene diamide derivative	Fluorimetry	–	13.8	1
8-Aminonaphthalene-1,3, 6-trisulfonate	Fluorimetry	1.0–10^4	0.24	41
Cysteine-modified gold nanoparticles	Colorimetry	1–40	0.8	21
Pectinase-protected gold nanoparticles	Colorimetry	4.85×10^{-9}–1.6×10^4	4.0×10^{-9}	This work

extent of PE-AuNPs aggregates has a higher absorbance ratio.

To obtain the optimum conditions of the colorimetric assay, the effect of the amounts of PE-AuNPs on A_{665}/A_{523} were first studied and the corresponding results were displayed in Fig. S2. The results demonstrate that the A_{665}/A_{523} obviously increases with the increase of PE-AuNPs dosage until it reaches the highest at 50 μL. Since PE-AuNPs solution is sol system, too large amounts of PE-AuNPs was not conducive to its stability. Thus, 50 μL PE-AuNPs was selected for the subsequent work.

The pH value of the system is a crucial factor that affects the degree of aggregation of PE-AuNPs. Hence, the effect of pH on the A_{665}/A_{523} of PE-AuNPs was investigated in the absence and presence of Mg^{2+}. As seen from Fig. S3, the A_{665}/A_{523} of PE-AuNPs without Mg^{2+} has negligible change over the pH range of 4.0–10.0, indicating that the PE-AuNPs are stable when pH > 4.0. However, the value of A_{665}/A_{523} is higher under pH 2.0 and 3.0, which indicates that the stability of PE-AuNPs is a bit poor in extremely acidic medium. With the addition of Mg^{2+} in the PE-AuNPs system, the result exhibits that the value of A_{665}/A_{523} is higher than that without Mg^{2+} over the pH range of 2.0–10.0. In addition, the value of A_{665}/A_{523} in the presence of Mg^{2+} reached maximum at pH 4.0. Therefore, pH 4.0 was chosen for Mg^{2+} detection.

To investigate the aggregation kinetics of PE-AuNPs in the presence of Mg^{2+}, the changes of A_{665}/A_{523} value with incubation time ranging from 30 s to 30 min were also studied as shown in Fig. S4. It can be found that the A_{665}/A_{523} value increases very rapidly with the incubation time varying from 30 s to 10 min and begins to tend to stable when the incubation time exceeds 10 min, which reflects that Mg^{2+} would easily cause the complete aggregation of PE-AuNPs within 10 min. Consequently, we choose 10 min as the incubation time for Mg^{2+} detection.

Table 2 Determination of Mg^{2+} in water samples using the proposed assay

Sample	Concentration of magnesium (μM)	RSD (n = 3) (%)	Concentration of magnesium added (μM)	Concentration of magnesium found (μM)	Recovery (%)	RSD (n = 3) (%)
Tap water 1	2.8×10^{-3}	3.5	4.6×10^{-3}	7.54×10^{-3}	103.2	2.3
Tap water 2	2.1×10^{-3}	2.0	4.6×10^{-3}	6.54×10^{-3}	96.5	1.7
Tap water 3	3.6×10^{-3}	3.8	4.6×10^{-3}	8.27×10^{-3}	101.6	3.9
River water 1	9.8×10^{-4}	2.5	4.6×10^{-3}	5.52×10^{-3}	98.7	1.1
River water 2	1.2×10^{-4}	3.3	4.6×10^{-3}	4.85×10^{-3}	102.8	3.2
River water 3	1.6×10^{-4}	2.7	4.6×10^{-3}	4.61×10^{-3}	96.7	2.8
Deionized water 1	–	–	4.6×10^{-9}	4.57×10^{-9}	99.3	2.5
Deionized water 2	–	–	4.6×10^{-7}	4.66×10^{-7}	101.4	1.4
Deionized water 3	–	–	4.6×10^{-5}	4.51×10^{-5}	97.9	3.3

Selectivity of the Colorimetric Assay

To determine the selectivity of the proposed colorimetric method against Mg^{2+}, other metal ions such as K^+, Li^+, NH_4^+, Cd^{2+}, Mn^{2+}, Ba^{2+}, Zn^{2+}, Pb^{2+}, Hg^{2+}, Ca^{2+}, Al^{3+}, Cu^{2+}, Fe^{3+}, Co^{2+}, Na^+, and Mg^{2+} were tested in the assay. In these tests, the concentrations of other metal ions were 10-fold higher than that of Mg^{2+} ion. As manifested in Fig. 5, both the corresponding UV-visible spectra and photographic images indicate that none of these metal ions could cause a conspicuous aggregation as Mg^{2+} did. Only Mg^{2+} ion effectively induced the aggregation of PE-AuNPs with a red-shift in the SPR peak from 523 to 665 nm, giving a color change from wine red to blue that could be observed with the naked eye. The results confirmed that proposed colorimetric assay has a perfect selectivity toward Mg^{2+} ion.

Colorimetric Detection of Mg^{2+} Ion

To testify the sensitivity of the proposed colorimetric assay, we tested several Mg^{2+} solutions which had concentrations between 4.85×10^{-9} μM and 1.6×10^4 μM. The absorption spectra of PE-AuNPs solutions and photographs of the corresponding solutions were recorded. As shown in Fig. 6a, upon increasing Mg^{2+} concentration, the UV–vis absorbance curves show red-shift and broaden gradually, and a peak emerges slowly at longer wavelength 665 nm. Meanwhile, the color of the PE-AuNPs solutions gradually changes from wine red to blue, the lowest detection concentration with the naked eye is 0.52 μM, which is 1000 times lower than the normal content of Mg^{2+} in the human body. The absorbance ratio (A_{665}/A_{523}) as a function of the concentration of Mg^{2+} is plotted in Fig. 6b, c. There were two good linear relationships between the A_{665}/A_{523} value and Mg^{2+} concentration over the ranges of 5.34×10^{-7} to 51.4 μM and 5.12×10^2 to 3.19×10^3 μM. And the correlated coefficient r^2 is 0.996 and 0.998, respectively. The relative standard deviation (RSD) is 3.0 % for six repeated measurements of 0.48 mM Mg^{2+}. The limit of detection (LOD) for Mg^{2+} ions at a signal-to-noise ratio (S/N) of 3 has been calculated to be 4.0×10^{-9} μM with UV–vis spectrophotometer, which is much lower than that of the other reported Mg^{2+} chemosensor methods [38–41] as shown in Table 1. Most importantly, compared with other methods for Mg^{2+} ion detection, this colorimetric assay shows not only better performance but also cost-effective and user- and eco-friendly property.

Analysis of Mg^{2+} in Real Samples

The proposed colorimetric assay was applied to Mg^{2+} determinations in several tap water, lake water, and deionized water samples, and the analytical results are listed in Table 2. Moreover, the recovery tests for Mg^{2+} were performed by adding known amounts of Mg^{2+} standards in the real samples. The amounts of added Mg^{2+} ion were then evaluated by using the proposed colorimetric assay. The results of recovery of the samples are also summarized in Table 2. The recovery values ranged from 96.5 to 103.2 %, with the relative standard deviation (RSD) lower than 3.9 %, revealing the present PE-AuNPs-based colorimetric assay can be used for detection Mg^{2+} in environmental samples. The recovery tests also demonstrate that the proposed colorimetric assay offers an excellent, accurate, and precise method for the determination of Mg^{2+} ion.

Conclusion

In summary, a simple and "green" approach for the synthesis of pectinase-protected gold nanoparticles has been developed for the first time. Moreover, the obtained PE-AuNPs was subsequently used as an ultra-sensitive and highly selective colorimetric assay for detection of Mg^{2+} ion. The study results show that Mg^{2+} can induce the aggregation of PE-AuNPs, which made a visual color change from red to blue and a red-shift in the SPR peak from 523 to 665 nm. The proposed colorimetric assay of Mg^{2+} could be operated by both the naked eye and UV–vis spectrophotometry. The lowest detection concentration with the naked eye is 0.52 μM. The detection limit is 4.0×10^{-9} μM with UV–vis spectrophotometer. The proposed Mg^{2+} detection assay offers several advantages compared with other reported methods. For instance, the Mg^{2+} recognition can be easily observed by eye and thus does not require advanced instruments. Moreover, the colorimetric assay also shows better performance, cost-effective, and user- and eco-friendly property. Our work provided a novel gold nanoparticles, which is a promising nanomaterials for colorimetric assay, and it can be extensively applied in bioanalysis and biomedical field.

Acknowledgments This work was supported by the National Natural Science Foundation of China (Nos. 21305082, 21306108, 21403135, 21575084, and 21475080), Program for the Outstanding Innovative Teams of Higher Learning Institutions of Shanxi, Research Project Supported by Shanxi Scholarship Council of China (No. 2014-017), Fund Program for the Scientific Activities of Selected Returned Overseas Professionals in Shanxi Province, and 131 Leading Talents Project of Higher Learning Institutions of Shanxi.

References

1. Song KC, Choi MG, Ryu DH, Kim KN, Chang SK (2007) Ratiometric chemosensing of Mg^{2+} ions by a calix[4] arene diamide derivative. Tetrahedron Lett 48:5397–5400
2. Saris NEL, Mervaala E, Karppanen H, Khawaja JA, Lewenstam A (2000) Magnesium. An update on physiological, clinical and analytical aspects. Clin Chim Acta 294:1–26

3. Hama H, Morozumi T, Nakamura H (2007) Novel Mg^{2+}-responsive fluorescent chemosensor based on benzo-15-crown-5 possessing 1-naphthaleneacetamidemoiety. Tetrahedron Lett 48: 1859–1861
4. Li L, Yuan Z, Peng X, Li L, He J, Zhang Y (2014) Highly selective colorimetric detection of copper ions using cysteamine functionalized gold nanoparticles. J Chin Chem Soc 61:1371–1376
5. Yang DY, Lee JB, Lin MC, Huang YL, Liu HW, Liang YJ, Cheng FC (2004) The determination of brain magnesium and zinc levels by a dual-probe microdialysis and graphite furnace atomic absorption spectrometry. J Am Coll Nutr 23:552S–555S
6. Durlach J, Bac P, Durlach V, Rayssiguier Y, Bara M, Guiet-Bara A (1998) Magnesium status and ageing: an update. Magnes Res 11: 25–42
7. Chung YT, Ling YC, Yang CS, Sun YC, Lee PL, Lin CY, Hong CC, Yang MH (2007) In vivo monitoring of multiple trace metals in the brain extracellular fluid of anesthetized rats by microdialysis membrane desalter-ICPMS. Anal Chem 79:8900–8910
8. Zhang Z, Zhao L, Lin Y, Yu P, Mao L (2010) Online electrochemical measurements of Ca^{2+} and Mg^{2+} in rat brain based on divalent cation enhancement toward electrocatalytic NADH oxidation. Anal Chem 82:9885–9891
9. Farruggia G, Iotti S, Prodi L, Montalti M, Zaccheroni N, Savage PB, Trapani V, Sale P, Wolf FI (2006) Hydroxyquinoline derivatives as fluorescent sensors for magnesium in living cells. J Am Chem Soc 128:344–350
10. Suzuki Y, Komatsu H, Ikeda T, Saito N, Araki S, Citterio D, Hisamoto H, Kitamura Y, Kubota T, Nakagawa J, Oka K, Suzuki K (2002) Design and synthesis of Mg^{2+}-selective fluoroionophores based on a coumarin derivative and application for Mg^{2+} measurement in a living cell. Anal Chem 74:1423–1428
11. Ishida M, Naruta Y, Tani F (2010) A porphyrin-related macrocycle with an embedded 1, 10-phenanthroline moiety: fluorescent magnesium(II) ion sensor. Angew Chem Int Ed 49:91–94
12. Prodi L, Bolletta F, Montalti M, Zaccheroni N, Savage PB, Bradshaw JS, Izatt RM (1998) A fluorescent sensor for magnesium ions. Tetrahedron Lett 39:5451–5454
13. Saha K, Agasti SS, Kim C, Li X, Rotello VM (2012) Gold nanoparticles in chemical and biological sensing. Chem Rev 112:2739–2779
14. Jans H, Huo Q (2012) Gold nanoparticle-enabled biological and chemical detection and analysis. Chem Soc Rev 41:2849–2866
15. Yuan Z, Lu F, Peng M, Wang CW, Tseng YT, Du Y, Cai N, Lien CW, Chang HT, He Y, Yeung ES (2015) Selective colorimetric detection of hydrogen sulfide based on primary amine-active ester cross-linking of gold nanoparticles. Anal Chem 87:7267–7273
16. Qian Q, Deng J, Wang D, Yang L, Yu P, Mao L (2012) Aspartic acid-promoted highly selective and sensitive colorimetric sensing of cysteine in rat brain. Anal Chem 84:9579–9584
17. Sener G, Uzun L, Denizli A (2014) Lysine-promoted colorimetric response of gold nanoparticles: a simple assay for ultrasensitive mercury(II) detection. Anal Chem 86:514–520
18. Liu D, Yang J, Wang HF, Wang Z, Huang X, Wang Z, Niu G, Hight Walker AR, Chen X (2014) Glucose oxidase-catalyzed growth of gold nanoparticles enables quantitative detection of attomolar cancer biomarkers. Anal Chem 86:5800–5806
19. Yuan Z, Cheng J, Cheng X, He Y, Yeung ES (2012) Highly sensitive DNA hybridization detection with single nanoparticle flash-lamp darkfield microscopy. Analyst 137:2930–2932
20. Lee JS, Han MS, Mirkin CA (2007) Colorimetric detection of mercuric ion (Hg^{2+}) in aqueous media using DNA-functionalized gold nanoparticles. Angew Chem Int Ed 46:4093–4096
21. Zhuang X, Wang D, Yang L, Yu P, Jiang W, Mao L (2013) Cysteine-modulated colorimetric sensing of extracellular Mg^{2+} in rat brain based on the strong chelation interaction between dithiothreitol and Mg^{2+}. Analyst 138:3046–3052
22. Bahram M, Mohammadzadeh E (2014) Green synthesis of gold nanoparticles with willow tree bark extract: a sensitive colourimetric sensor for cysteinedetection. Anal Methods 6:6916–6924
23. Tsuji M, Hashimoto M, Nishizawa Y, Kubokawa M, Tsuji T (2005) Microwave-assisted synthesis of metallic nanostructures in solution. Chem Eur J 11:440–452
24. Vargas-Hernandez C, Mariscal MM, Esparza R, Yacaman MJ (2010) A synthesis route of gold nanoparticles without using a reducing agent. Appl Phys Lett 96:213115/1–213115/3
25. Housni A, Ahmed M, Liu S, Narain R (2008) Monodisperse protein stabilized gold nanoparticles via a simple photochemical process. J Phys Chem C 112:12282–12290
26. Higashi N, Kawahara J, Niwa M (2005) Preparation of helical peptide monolayer-coated gold nanoparticles. J Colloid Interface Sci 288:83–87
27. Tomuleasa C, Soritau O, Orza A, Dudea M, Petrushev B, Mosteanu O, Susman S, Florea A, Pall E, Aldea M, Kacso G, Cristea V, Berindan-Neagoe I, Irimie A (2012) Gold nanoparticles conjugated with cisplatin/doxorubicin/capecitabine lower the chemoresistance ofhepatocellular carcinoma-derived cancer cells. J Gastrointestin Liver Dis 21:187–196
28. Tan YN, Lee JY, Wang DI (2010) Uncovering the design rules for peptide synthesis of metal nnanoparticles. J Am Chem Soc 132: 5677–5686
29. Gedye R, Smith F, Westaway K, Ali H, Baldisera L, Laberge L, Rousell J (1986) The use of microwave ovens for rapid organic synthesis. Tetrahedron Lett 27:279–282
30. Giguere RJ, Bray TL, Duncan SM (1986) Application of commercial microwave ovens to organic synthesis. Tetrahedron Lett 27: 4945–4948
31. Beeri A, Berman E, Vishkautsan R, Mazur Y (1986) Reactions of hydrogen atoms produced by microwave discharge with olefins in acetone and toluene. J Am Chem Soc 108:6413–6414
32. Liu X, Atwater M, Wang J, Huo Q (2007) Extinction coefficient of gold nanoparticles with different sizes and different capping ligands. Colloids Surfaces B 58:3–7
33. Sun C, Yang H, Yuan Y, Tian X, Wang L, Guo Y, Xu L, Lei J, Gao N, Anderson GJ, Liang X, Chen C, Zhao Y, Nie G (2011) Controlling assembly of paired gold clusters within apoferritin nanoreactor for in vivo kidney targeting and biomedical imaging. J Am Chem Soc 133:8617–8624
34. Mehta VN, Singhal RK, Kailasa SK (2015) A molecular assembly of piperidine carboxylic acid dithiocarbamate on gold nanoparticles for the selective and sensitive detection of Al^{3+} ion in water samples. RSC Adv 5:33468–33477
35. Maity D, Gupta R, Gunupuru R, Srivastava DN, Paul P (2014) Calix[4]arene functionalized gold nanoparticles: application in colorimetric and electrochemical sensing of cobalt ion in organic and aqueous medium. Sensors Actuators B Chem 191:757–764
36. He Y, Liang Y, Song H (2015) One-pot preparation of creatinine-functionalized gold nanoparticles for colorimetric detection of silver ions. Plasmonics. doi:10.1007/s11468-015-0092-2
37. Cao XH, Zhang HY, Ma RC, Yang Q, Zhang ZB, Liu YH (2015) Visual colorimetric detection of UO_2^{2+} using o-phosphorylethanolamine-functionalized gold nanoparticles. Sensors Actuators B Chem 218:67–72
38. Xie J, Zheng Y, Ying J (2009) Protein-directed synthesis of highly fluorescent gold nanoclusters. J Am Chem Soc 131: 888–889
39. Komatsu H, Miki T, Citterio D, Kubota T, Shindo Y, Kitamura Y, Oka K, Suzuki KJ (2005) Single molecular multianalyte (Ca^{2+}, Mg^{2+}) fluorescent probe and applications to bioimaging. Am Chem Soc 127:10798–10799

40. Capitan-Vallvey LF, Fernandez-Ramos MD, Lapresta-Fernandez A, Brunet E, Rodrıguez-Ubis JC, Juanes O (2006) Magnesium optical one-shot sensor based on a coumarin chromoionophore. Talanta 68:1663–1670

41. Jin L, Guo Z, Sun Z, Li A, Jin Q, Wei M (2012) Assembly of 8-aminonaphthalene-1,3,6-trisulfonate intercalated layered double hydroxide film for the selectivedetection of Mg^{2+}. Sensors Actuators B Chem 161:714–720